

QUANTITATIVE ANALYSIS OF MULTIPOLE ERRORS INDUCED BY MECHANICAL DEFORMATIONS OF AN UNDULATOR

T.Y. Chung[†], C.H. Chang, H.W. Luo, C.S. Hwang
 National Synchrotron Radiation Research Center, Hsinchu, Taiwan

Abstract

To minimize unwanted beam dynamics effects in a storage ring, multipole errors in an undulator are normally reduced by sorting and shimming methods. Nonetheless, an investigation of the error source is worth pursuing and interesting. Our work focuses on multipole errors introduced by mechanical deformations of an APPLE-II type undulator, which undergoes complicated forces during operation. Our results give guidelines for mechanical specifications derived from quantitative analyses.

INTRODUCTION

An undulator is typically used to serve as a high brightness synchrotron radiation source in a photon facility. The desired undulator must have a negligible effect on beam dynamics. In practice, misalignment of mechanical structures or non-identical magnets contribute to imperfect and non-periodic magnetic fields, leading to a decrease in the photon flux and ill effects on electron beam dynamics. While magnet shimming methods are effective during construction [1], it seems more suitable to analyze and reduce errors early on.

An undulator normally consists of two magnet arrays, one above and one below the electron beam. The APPLE-II [2] type undulator has a more complicated mechanical structure. To produce variable magnetic field polarizations, the magnets in an APPLE-II are split resulting in four magnet arrays, two above and two below the beam axis, as seen in Fig. 1. The horizontal gap (G_h) between nearby magnet arrays is typically 1 mm to allow for mechanical movement of the arrays to change its magnetic field polarization. The narrow gap, however, creates strong magnetic forces. Various operation modes of the APPLE-II generate magnetic force conditions, which transform the undulator into a complicated mechanical deformation system.

To minimize their effect on storage ring operation, people focus mainly on undulator multipole field errors and develop various correction methods. Coupling effects on the beam attract special attention because they are more difficult to correct [3] and observed especially in an APPLE-II [4-7]. To determine the field quality in an undulator, the magnetic field is expressed as a complex quantity defined by the following equation.

$$\int_{-\infty}^{\infty} dz (B_x(x, y) + iB_y(x, y)) \equiv \sum_{n=0}^{\infty} (a_n + ib_n)(x + iy)^n$$

[†] chung.albert@nsrc.org.tw

Here B_y and B_x are the vertical and horizontal field components, and the field integral is taken over the length of the undulator. The coefficients a_n and b_n are the skew and normal field components and the index n is the multipole order e.g. dipole ($n=0$), quadrupole ($n=1$), sextupole ($n=2$), octupole ($n=3$), decapole ($n=4$). Finally, the location of the electron beam axis is defined by $x = y = 0$ and the multipole expansion in this note is done in the midplane at $y = 0$.

The typical structure of an APPLE-II and its parts definitions are shown in Fig. 1. A magnet block is held by a keeper, which is mounted on a sliding beam. Four sliding beams, guided by linear guide rails, allow longitudinal movement of the magnet arrays. The whole structure is supported by a strong-back or girder, which can be moved by a mechanical system to vary the gap size. A C-type frame, allowing for installation of vacuum chambers, supports the whole assembly.

The multipole errors induced by the mechanical deformation of each part are studied and simulated using the Radia code [8]. In this study, the parameters of the APPLE-II for the magnetic field and magnetic force are given by the magnet block: $H \times V \times L = 45 \times 32 \times 16.5 \text{ mm}^3$ and $B_r = 1.24 \text{ T}$. We organize this paper as follows. In Section 2, we discuss multipole errors generated by the deformation of the girder and frame. The effects from the sliding beam and keeper are then discussed in Sections 3 and 4. Section 4 also gives solutions to eliminate major error sources. A summary is given in Section 5.

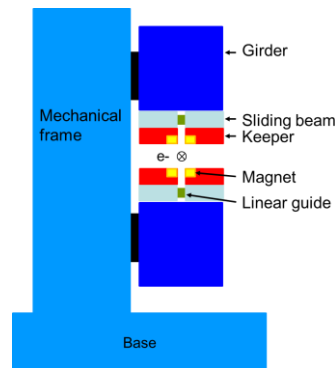


Figure 1: A typical structure of an APPLE-II undulator.

FRAME AND GIRDER DEFORMATION

The magnetic forces between upper and lower girder are shown in Fig. 2. The longitudinal and horizontal forces nearly cancel, while the vertical force changes sign as the phase is changing. During operation, the girder and frame are under attractive and/or repulsive forces. The bending of

This is a preprint — the final version is published with IOP

Content from this work may be used under the terms of the CC BY 3.0 licence (© 2018). Any distribution of this work must maintain attribution to the author(s), title of the work, publisher, and DOI.

Content from this work may be used under the terms of the CC BY 3.0 licence (© 2018). Any distribution of this work must maintain attribution to the author(s), title of the work, publisher, and DOI.

the mechanical frame and other mechanical imperfections cause a non-parallelism between the magnets, as seen in the sketch of Fig. 2. To demonstrate the effect on the multipole errors, a model of a 2 m long APPLE-II was studied. The magnet blocks in the model create a normal dipole with a strength and angle tolerance of $\pm 1\%$ and $\pm 1^\circ$, respectively. These values are typical specifications for the magnet blocks. Deformations, as shown in the sketch of Fig. 2, can introduce multipole errors as shown in Fig. 3 where the normal and skew components change linearly for small angle variations as the angular deformation changes. The slope of each curve will be summarized in Table 1.

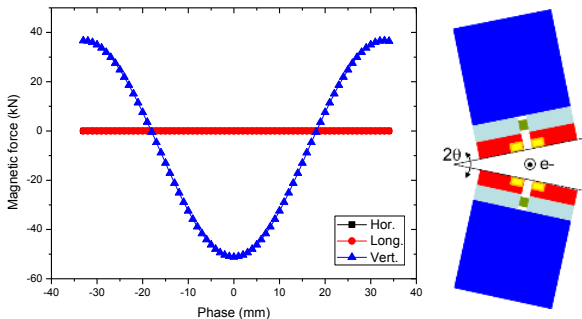


Figure 2: Magnetic force calculation on one girder for various phases with horizontal (square), longitudinal (circle) and vertical (triangle) force components. The sketch shows a non-parallel deformation.

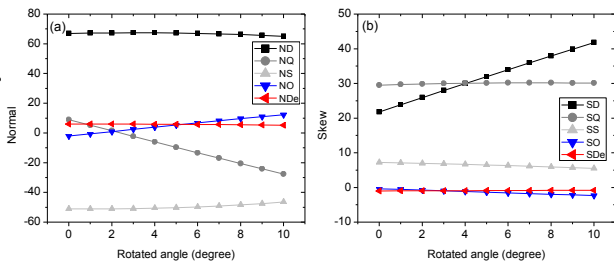


Figure 3: Multipole components induced by an angular deformation of the girder. Normal (a) and skew components (b) are labeled by the corresponding dipole (D), quadrupole (Q), sextupole (S), octupole (O) and decapole (De). The unit for the dipole, quadrupole, sextupole, octupole and decapole is presented in an integral form as $Gcm/(cm)^n$.

SLIDING BEAM DEFORMATION

The magnetic forces within the arrays are calculated for various phase modes. Figure 4 shows that the horizontal and vertical forces at phase = 0 and over ± 33 mm reach extreme values with changing signs. The forces act on the arrays so as to rotate around the linear girder. Analysing the magnetic forces of four arrays, the deformation of the four arrays are shown in the sketch of Fig. 4. The angular deformation of the four arrays, whether far or close to the electron beam, depend on the actual phase. A multipole analysis as a function of the rotational angle is also done, as seen in Fig. 5. An almost linear behavior is observed and the slopes of each curve will be summarized in the Table 1.

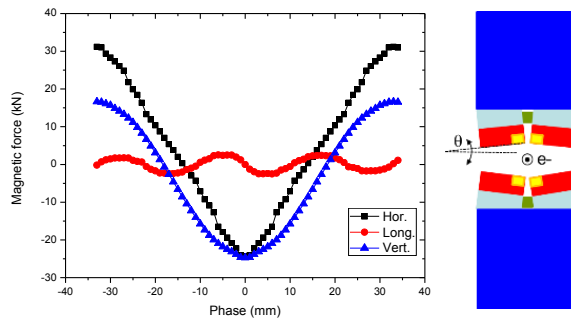


Figure 4: Magnetic force calculation of one array for various phases and horizontal (square), longitudinal (circle) and vertical (triangle) force components. The sketch shows the deformations of the four arrays schematically.

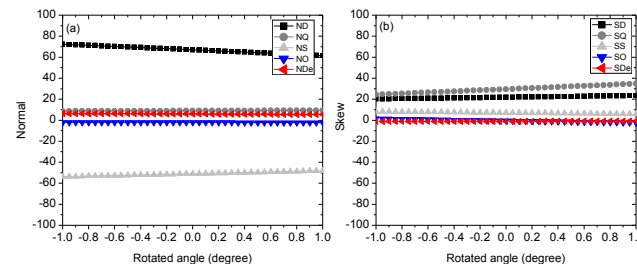


Figure 5: Multipole field components induced by a rotation of four sliding beams.

KEEPER DEFORMATION

The magnetic forces on a single block are large even when the vertical gap is fully open. During operation of the APPLE-II, magnetic fields act on each block with variable strength and direction. Figure 6(a) shows the magnetic forces of vertically and horizontally magnetized blocks. A strong vertical force is obvious for both kinds. A phase-dependent behavior can also be observed for the longitudinal and horizontal force even though they are smaller than for the vertical force. A complete simulation and analysis, reveals that two kinds of rotation on the vertical and horizontal blocks can create significant multipole errors, as seen in Figs. 6(b) and 6(c).

The process of simulation and analysis are similar to that shown in Figs. 3 and 5. A nearly linear behavior is still observed and characterized by a slope, which represents the degree the deformation has on multipole errors. Table 1 summarizes the slope of each multipole induced by major deformations as considered. A block rotation caused by a keeper deformation is the major error source, especially for dipole, quadrupole and sextupole errors. A cancellation of ND, SD and SS occurs due to the contribution from a reversed sign in the rotation of vertical and horizontal blocks. The NQ and SQ errors, however, are still obvious. A keeper design that can withstand magnetic forces is therefore critical to suppress multipole errors even though the allowable values for each multipole depend on the tolerances of the facility.

This is a preprint — the final version is published with IOP

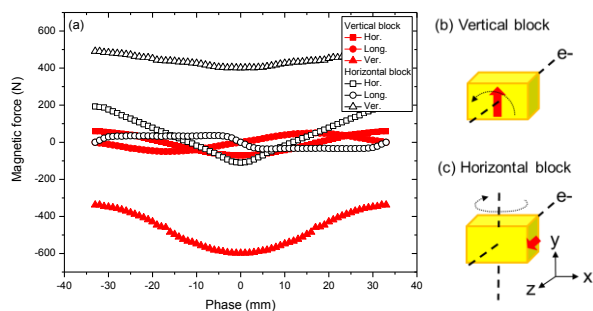


Figure 6: (a) Force calculations for two types of magnet blocks in various phases, where vertical blocks are marked (solid) and horizontal blocks (open) and for horizontal (square), longitudinal (circle) and vertical (triangle) force components. Two types of block rotation, vertical (b) and horizontal (c) along the axis are shown by the dashed arrow. The solid arrow indicates the magnetization direction.

Table 1: Summary of Multipole Errors Induced by Deformations of Mechanical Parts

	Unit	Backing beam	Sliding beam	V_block along Z	H_block along Y
ND	Gcm/deg	0	-5	-47	72
NQ	Gcm/cm deg	-4	0	-115	2
NS	Gcm/cm ² deg	0	3	38	-25
NO	Gcm/cm ³ deg	1	0	58	2
NDe	Gcm/cm ⁴ deg	0	0	-8	3
SD	Gcm/deg	2	2	-92	52
SQ	Gcm/cm deg	0	5	58	3
SS	Gcm/cm ² deg	0	-1	73	-14
SO	Gcm/cm ³ deg	0	-2	-36	0
SDe	Gcm/cm ⁴ deg	0	0	-13	28

Reducing magnetic forces and increasing the stiffness of the keeper are considered to minimize its deformation. The magnetic forces are related to the magnetic fields and to the dimensions of the blocks. Generally, a trade-off between the size of a block and G_h with the homogeneity of the magnetic field is preferred to reduce the effects on beam dynamics. Another way to decrease the load on the keeper is to glue vertical and horizontal blocks to one keeper. An exotic magnetization process on the blocks exists to optimize the equivalent magnetic fields [9], but the efficacy of the method strongly relies on the technical ability of the magnet manufacturer.

The stiffness of a keeper can be enhanced by materials with a large Young's modulus, such as stainless steel [10] rather than the generally used aluminum to manufacture a keeper. Any residual magnetic hysteresis of steel must, however, be carefully eliminated after machining. A dedicated design of the keeper to achieve the desired results is proposed here and a typical structure is shown in Fig. 7. A block is fixed by two screws on a keeper and can be adjusted vertically and horizontally using a wedge for virtual shimming [11]. When the keeper deforms during operations, a rotation and deviation of a block occurs, as seen in the mechanical analysis (Fig. 7). The deformation is 67 μm for the model in our calculation. A straightforward improvement can be made with a fixed screw on the bottom of the magnet to limit the keeper deformation. Figure 8 shows such a design and the deformation is reduced to within 10 μm . Although the after-assembly improvement is very effective, an efficient block sorting and shimming

algorithm should be followed for construction to minimize the need for after-assembly adjustments.

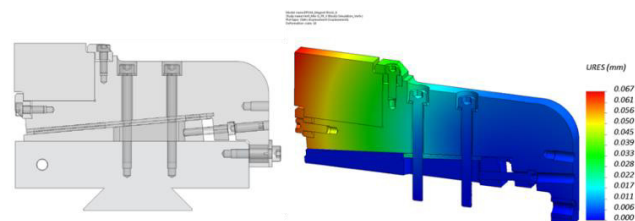


Figure 7: A typical structure and mechanical deformation analysis of the keeper without a fixed screw.

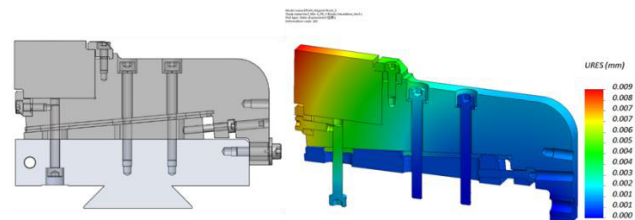


Figure 8: A robust structure and mechanical deformation analysis of the keeper with a fixed screw.

DISCUSSION

This work analyzes multipole errors introduced from mechanical deformations of major undulator parts. Deformations of the frame, girder and sliding beams are not critical to cause multipole errors. The main error source comes from keeper deformations. A solution to increase the stiffness of a keeper is offered based on an extra fixed screw design. The results of this study can serve as a mechanical guideline and to manage tolerances during the design of undulators.

ACKNOWLEDGEMENTS

This work was supported in part by the Ministry of Science and Technology of Taiwan under contract MOST106-2112-M-213-004.

REFERENCES

- [1] J. Bahrtdt *et al.*, *Nucl. Instr. and Meth. A*, 516, 575 (2004).
- [2] S. Sasaki, *Nucl. Instr. and Meth. A*, 347, 86 (1994).
- [3] A. Franchi *et al.*, *Phys. Rev. ST Accel. Beams* 14, 034002 (2011).
- [4] C. Steier *et al.*, Proc. of EPAC'04, Lucerne, Switzerland, Jul. 2004, paper MOPKF071, pp. 479-481.
- [5] S. Marks *et al.*, *IEEE Transactions on Applied Superconductivity*, 16, 1574-77 (2006).
- [6] T. Kaneyasu *et al.*, *Nucl. Instrum. Methods Phys. Res. A* 641, 5 (2011).
- [7] T.Y. Chung *et al.*, *Nucl. Instrum. Methods Phys. Res. A* 826, 48 (2016).
- [8] O. Chubar, P. Elleaume, J. Chavanne, *Synchrotron Radiat.* 5, 481 (1998).
- [9] E. Wallén *et al.*, Proc. of IPAC'14, Dresden, Germany, June 2014, paper TUPRO103, pp. 1286-1288.

Content from this work may be used under the terms of the CC BY 3.0 licence (© 2018). Any distribution of this work must maintain attribution to the author(s), title of the work, publisher, and DOI.

- [10] F. Briquez *et al.*, Proc. of FEL'08, Gyeongju, Korea, Aug. 2008, paper TUPPH015, pp. 265-268.
- [11] T.Y. Chung *et al.*, Synchrotron Radiat. News, 28, 29 (2015).